BIOCHEMISTRY
including biophysical chemistry & molecular biology
Article

Biochemistry **2009,** *48,* 6975–6987 6975
DOI: 10.1021/bi900641c

The Core Signaling Proteins of Bacterial Chemotaxis Assemble To Form an Ultrastable Complex[†]

Annette H. Erbse and Joseph J. Falke*

Department of Chemistry, and Biochemistry and Molecular Biophysics Program, University of Colorado, Boulder, Colorado 80309-0215

Received April 15, 2009; Revised Manuscript Received May 19, 2009

ABSTRACT: The chemosensory pathway of bacterial chemotaxis forms a polar signaling cluster in which the fundamental signaling units, the ternary complexes, are arrayed in a highly cooperative, repeating lattice. The repeating ternary units are composed of transmembrane receptors, histidine-kinase CheA, and coupling protein CheW, but it is unknown how these three core proteins are interwoven in the assembled ultrasensitive lattice. Here, to further probe the nature of the lattice, we investigate its stability. The findings reveal that once the signaling cluster is assembled, CheA remains associated and active for days in vitro. All three core components are required for this ultrastable CheA binding and for receptor-controlled kinase activity. The stability is disrupted by low ionic strength or high pH, providing strong evidence that electrostatic repulsion between the highly acidic core components can lead to disassembly. We propose that ultrastability arises from the assembled lattice structure that establishes multiple linkages between the core components, thereby conferring thermodynamic or kinetic ultrastability to the bound state. An important, known function of the lattice structure is to facilitate receptor cooperativity, which in turn enhances pathway sensitivity. In the cell, however, the ultrastability of the lattice could lead to uncontrolled growth of the signaling complex until it fills the inner membrane. We hypothesize that such uncontrolled growth is prevented by an unidentified intracellular disassembly system that is lost when complexes are isolated from cells, thereby unmasking the intrinsic complex ultrastability. Possible biological functions of ultrastability are discussed.

Chemotactic bacteria regulate their motility to swim up or down concentration gradients of chemical attractants or repellents, respectively. In *Escherichia coli* and *Salmonella typhimurium*, extracellular attractants and repellents are sensed by the periplasmic domains of transmembrane chemoreceptors. The receptors first form stable homodimers, which then combine in trimers of dimers (*1*−*5*). Thousands of trimers of dimers, in turn, assemble into an ordered array at the cell pole, yielding a structural framework to which all cytoplasmic components of the chemosensory pathway dock (*6*−*10*). Within the assembled signaling lattice, ligand binding generates highly cooperative on−off signals that regulate the kinase activity of multiple receptor−CheA−CheW ternary complexes (*11*, *12*). Periplasmic attractant binding triggers a "kinase-off" signal by transmitting a long-range, transmembrane conformational change through the receptor to the CheA kinase, which is bound to the receptor cytoplasmic domain (*5*, *13*−*15*). Adaptation sites on the receptor cytoplasmic domain also regulate kinase activity, generating a "kinase-on" signal when covalently modified by the adaptation enzyme CheR (*16*). The receptor integrates these attractant and adaptation signals to control the net kinase activity of CheA. Ultimately, CheA kinase activation produces phospho-CheY, which dissociates from the signaling lattice and diffuses through the cytoplasm to the flagellar motor, thereby modulating cell motility (*1*, *2*, *17*, *18*).

It has long been argued that strong positive cooperativity between multiple proteins in local regions of the signaling lattice is essential for the remarkable ultrasensitivity of the chemosensory pathway, which efficiently guides chemotaxis in attractant concentrations spanning 4 orders of magnitude (*11*, *19*−*23*). The recent structural studies of the assembled signaling lattice support the idea that direct, protein−protein contacts in an extensive lattice network drive this cooperativity (*7*, *8*). In principle, such networking could also lead to high lattice stability as all the components snap into place, much like the enhanced structural integrity observed for a fully assembled jigsaw puzzle. To test the latter new hypothesis, this study investigates the stability of the assembled signaling lattice. The results indicate that as long as the lattice is formed from all three components, it is ultrastable in vitro. We propose this stability arises from networked protein−protein interactions systematically linking CheA, CheW, and the cytoplasmic tips of receptor dimers, both within and between adjacent trimers of dimers.

[†]Support provided by National Institutes of Health Grant R01 GM-040731 (to J.J.F.).

*To whom correspondence should be addressed. E-mail: falke@colorado.edu. Telephone: (303) 492-3503. Fax: (303) 492-5894.

© 2009 American Chemical Society

Published on Web 05/20/2009

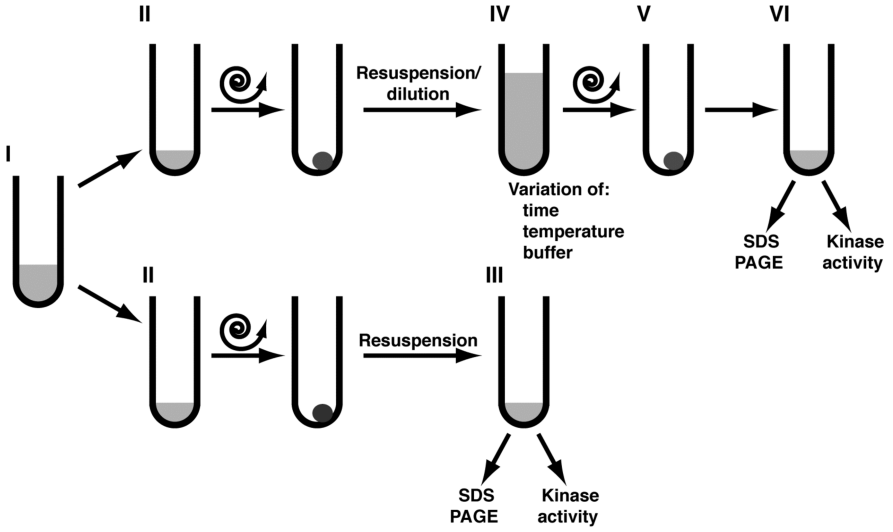

FIGURE 1: Analysis of signaling complex stability and experimental design. In vitro-reconstituted or ex vivo-isolated (see Materials and Methods) membrane-associated complexes (step I) were separated from unbound components by pelleting and removal of supernatant (step II). Half the pellet was resuspended to half the original volume in activity buffer and assayed for the baseline CheA:receptor ratio as determined by SDS−PAGE, and for the baseline receptor-regulated CheA activity as determined by a standard kinase assay (step III). The other half-pellet was resuspended in a large volume of a variable buffer, followed by incubation to challenge with various test conditions for a defined length of time (step IV). The challenged complexes were re-isolated (step V) and resuspended to the original volume in activity buffer prior to carrying out the two aforementioned assays (step VI). Together, steps II−VI provided a 100−500-fold dilution factor, ensuring that free proteins were effectively removed prior to final assays.

MATERIALS AND METHODS

Materials. Reagents were obtained from the following sources: [γ-^{32}P]ATP from Perkin-Elmer and all other reagent grade chemicals from Sigma unless noted otherwise.

Protein Expression and Purification. Cysless *S. typhimurium* CheA and CheW proteins were expressed with N-terminal six-His tags from plasmids pET6H-CheA and pET6H-CheW (*24*); N-terminal six-His-tagged *S. typhimurium* CheR was expressed from plasmid pET6H-CheR [constructed from pET28 (this work)]. Six-His-tagged *E. coli* CheY was expressed from plasmid pVSCheY-6H (*25*). All His-tagged proteins were isolated by standard Ni-NTA affinity chromatography. Protein concentrations were estimated by UV absorption. Extinction coefficients at 276 nm of 16.0 for CheA, 5.95 for CheW, and 32.4 for CheR and at 280 nm of 6.97 (mM^{-1} cm^{-1}) for CheY were calculated from the protein sequences.

The *S. typhimurium* aspartate receptor (Tar) was expressed from plasmid pSCF6 (*26*) in strain RP3808. The *E. coli* serine receptor (Tsr) was expressed from plasmid pJC3 (*27*) in strain RP3098. Tar-containing membranes and Tsr-containing inner membranes were isolated as described previously (*24*, *28*). The total protein content of the membranes was determined with the BCA assay using BSA as a standard. The percentage of receptor in the membranes was determined by SDS−PAGE.[1] Receptor bands were imaged with a digital camera and analyzed with integration software (Alpha Inotech).

Ex Vivo Isolation of Membrane-Associated, Functional Signaling Complexes. *E. coli* Tsr from plasmid pJC3 was coexpressed with wild-type (wt) *E. coli* CheA and CheW from plasmid pPM23 with the nonperturbing mutation CheA Ay2v (*9*) (originally from J. S. Parkinson, University of Utah, Salt Lake City, UT) in strain RP3098 to assemble signaling complexes in cells. Bacteria were grown in LB broth with ampicillin (25 μg/mL), chloramphenicol (15 μg/mL), and 1 μM sodium salicylate to induce CheA and CheW. pJC3 was not induced to keep the level of overexpression of Tsr as low as possible. Bacteria were grown at 30 °C and harvested at an OD of 1.2. Bacterial pellets were resuspended in high-salt buffer [20 mM sodium phosphate (pH 7.0), 2 M KCl, 10% glycerol, 10 mM EDTA, 5 mM DTT, 0.5 mM PMSF, and 2.5 mM 1,10-phenanthroline]. Lysozyme (1 mg/mL) was added, and the resuspension was incubated on ice for 30 min. Bacteria were further lysed by sonication in an ice/NaCl/water bath. After sonication, unbroken cells and particulate matter were removed by centrifugation (12000*g* for 20 min). Membranes were then pelleted by ultracentrifugation (450000*g* for 15 min) and resuspended in high-salt buffer without 1,10-phenanthroline by sonication. Subsequently, membranes were pelleted, resuspended in activity buffer [50 mM Tris-HCl (pH 7.5), 10% glycerol, 0.5 mM EDTA, 160 mM NaCl, 5 mM $MgCl_2$, and 0.5 mM PMSF], and pelleted again. Finally, membranes were resuspended in a small volume of activity buffer, frozen in liquid nitrogen, and stored at −70 °C.

In Vitro Reconstitution of Membrane-Associated, Functional Signaling Complexes. To reconstitute signaling complexes in vitro, 6.7 μM receptor in membranes was mixed with 5 μM CheA and 10 μM CheW in activity buffer with fresh PMSF and incubated for 45 min at 22 °C. Samples were centrifuged for 15 min at 180000*g* and 22 °C, and supernatants were removed. Pellets were resuspended in the appropriate buffer (see Figure 1).

Determination of the CheA:Receptor Ratio. To measure the relative CheA:receptor ratio of the Tsr-IM-in vitro complex, we mixed samples with SDS sample buffer and subjected the mixtures to 13.5% SDS−PAGE followed by Coomassie staining. Receptor and CheA bands were imaged with a digital camera and analyzed with integration software (Alpha Inotech). To measure the quantitative CheA:receptor ratio of all three different types of

[1]Abbreviations: DTT, dithiothreitol; EDTA, ethylenediaminetetraacetic acid; PMSF, phenylmethanesulfonyl fluoride; Ni-NTA, nickel-nitrilotriacetic acid, nickel-charged resin; IM, inner membrane; SM, sonication membrane; SDS−PAGE, sodium dodecyl sulfate−polyacrylamide gel electrophoresis; FRAP, fluorescence recovery after photobleaching; YFP, yellow fluorescent protein.

complexes, samples were Western blotted using polyclonal primary antibodies against Tsr (a gift from J. S. Parkinson) and CheA (a gift from J. Stock) and alkaline phosphatase-coupled secondary antibodies (Sigma).

To quantify the amount of CheA that could possibly become trapped in membrane pellets during centrifugation of the in vitro-reconstituted complexes, membranes without receptor were prepared and mixed with CheA and CheW and treated as described for in vitro complex reconstitution. The membrane samples were centrifuged as usual, dissolved in SDS loading buffer, and subjected to a Western blot against CheA. No trapped CheA was detected.

The accessibility of the cytoplasmic protein docking sites of Tsr and Tar to exogenously added proteins was estimated by measuring the availability of glutamates in the adaptation region for methylation by the CheR methyltransferase as described previously (*29*). As judged from the shifted mobility of the receptor bands, the accessibility was 80% of the receptor population in the Tsr-IM-in vitro preparations and 50% of the receptor population in the Tar-SM-in vitro and Tsr-ex vivo preparations. For the in vitro preparations, only the receptor concentration accessible to methylation was used to calculate the CheA:receptor ratio since only these receptors are accessible to added CheA and CheW for complex formation.

Analysis of Receptor-Regulated CheA Kinase Activity. The relative receptor-regulated kinase activity of the different signaling complexes (Figure 1A, steps III and IV) was measured as previously described (*26*) with the following modifications. Four microliters of the resuspended complex was mixed with 5 μL of activity buffer containing 20 μM CheY in the presence or absence of 2 mM attractant. Excess CheY ensured that CheA autophosphorylation was rate-determining, not phospho-transfer to CheY. Kinase reactions were initiated by the addition of [γ-^{32}P]ATP (4000−8000 cpm/pmol) to a final concentration of 1 mM. We quenched reactions after 10 s by mixing the samples with 30 μL of 2× Laemmli sample buffer containing 40 mM EDTA at 22 °C. Samples were immediately analyzed by SDS−PAGE, or during long time experiments, samples were snap-frozen in liquid nitrogen and stored at −80 °C and then thawed at 22 °C immediately prior to SDS−PAGE. Gels were dried, and the amount of phospho-CheY was quantitated by phosphorimaging.

The relative activities of the three different complexes per micromolar CheA or micromolar receptor were measured by mixing 4 μL of resuspended complexes with 5 μL of activity buffer containing 20 μM CheY. The reactions were started as described above and quenched after 6, 10, 15, and 20 s, and the mixtures were processed as described. The relative activity per unit concentration of CheA or receptor was determined by dividing the best-fit slope by the CheA or receptor concentration in the sample, both measured by quantitative Western blotting.

To measure equilibrium exchange of CheA incorporated into signaling complexes with an excess of a kinase-inactive CheA H69Q/G470K mutant or excess CheW, complexes were assembled by incubating membranes containing 4 μM Tar or Tsr in 50 mM Tris-HCl (pH 7.5), 160 mM NaCl, and 5 mM $MgCl_2$ with purified CheW (0.5 μM), CheA (0.5 μM), and CheY (20 μM) at room temperature for 45 min. Subsequently, without any further purification of the formed complexes, 50 μM CheA H68Q/G470K or CheW was added. Aliquots (10 μL) were removed at different time points, and reactions were started as described above.

Competition Assay between Active CheA and H48Q/G470K CheA. In vitro complexes were assembled from 4 μM receptor in membranes, 0.5 μM CheW, and 0.5 μM active CheA in the presence of increasing amounts of the kinase-inactive CheA mutant H48Q/G470K. Kinase activities were measured after incubation for 45 min at room temperature without isolating the complexes.

RESULTS

Assembly, Isolation, and Characterization of Signaling Complexes. Our studies analyzed the stabilities of three different types of lattices, assembled in different ways from the three core components and hereafter termed signaling complexes. Each of the chosen signaling complexes possessed unique experimental advantages and disadvantages. First, highly overexpressed *E. coli* serine receptor (Tsr) was isolated in *E. coli* inner membranes (*28*) (Tsr-inner membranes, Tsr-IM) and then incubated with purified, His-tagged, Cysless *S. typhimurium* soluble components (CheA and CheW) to assemble the Tsr-IM-in vitro complex. While subtle perturbations due to trans-species composition are possible, studies of trans-species complexes in cells have indicated that the *E. coli* and *S. typhimurium* components are functionally interchangeable (*30*). The resulting reconstituted signaling complex provided the highest density of active, assembled CheA kinase proteins, due to (i) the high receptor expression level and (ii) the inside-out nature of isolated inner membranes (*28*) that favorably orients the receptor cytoplasmic domains toward externally added CheA and CheW. However, the high levels of receptor overexpression in this system have been shown to yield nonphysiological receptor aggregates ("zippers") that may confer non-native properties (*31*, *32*). Therefore, we also tested a second in vitro signaling complex in which the *S. typhimurium* aspartate receptor (Tar) was assembled with purified, His-tagged, Cysless CheA and CheW of the same species (*13*). In this procedure, the receptor was only slightly overexpressed and was isolated in bacterial membranes by sonication (Tar-sonicated membranes, Tar-SM) prior to reconstitution. The resulting Tar-SM-in vitro complex eliminated any potential trans-species perturbations, and lower receptor expression levels minimized zipper formation (*9*). The third type of signaling complex, developed for this study, was assembled under native conditions in live cells by coexpressing wild-type *E. coli* receptor, CheA, and CheW at near-native expression levels. Previous cryo-EM studies have documented these conditions yield a nativelike, polar signaling complex with little or no zipper formation (*9*). The resulting complex was then isolated in bacterial membranes by a sonication protocol, yielding a new experimental system we term the Tsr-ex vivo complex. A disadvantage of the near-native expression level was a correspondingly lower membrane density of receptor-regulated CheA kinase.

All three signaling complexes displayed attractant-dependent, receptor-regulated CheA kinase activities, indicating they were correctly assembled and functional. Table 1 summarizes the key characteristics of each complex, measured after the membrane-bound complex had been washed to remove free components. The approximate CheA:receptor stoichiometry was determined by quantitative Western blotting and was corrected for the fraction of receptor accessible to CheR methylation, thereby eliminating contributions from receptor cytoplasmic domains hidden inside vesicles. In addition, relative CheA kinase activities were determined per total CheA and per accessible receptor,

Table 1: Characteristics of Three Types of Signaling Complexes

complex	components		receptor expression	assembly, isolation	CheA per receptor[a]	relative kinase activity per CheA[b]		relative kinase activity per receptor[b]	
	CheA, CheW	receptor				(−) attr	(+) attr	(−) attr	(+) attr
Tsr-IM-in vitro	His-tagged, Cysless *S. typhimurium*	*E. coli* Tsr	+ + + +	in vitro, osmotic	1:9 to 1:5	100 ± 5%	±2%	100 ± 20	5 ± 2%
Tar-SM-in vitro	His-tagged, Cysless *S. typhimurium*	*S. typhimurium* Tar	+ +	in vitro, sonication	1:9 to 1:6	120 ± 30	< 1[c]	100 ± 20	< 1[c]
Tsr-ex vivo	WT *E. coli*	*E. coli* Tsr	+	in vivo, sonication	1:8 to 1:4	30 ± 10	< 1[c]	80 ± 20	< 1[c]

[a] Approximate stoichiometry based on best estimates of the total CheA and accessible receptor concentrations (see Materials and Methods). [b] Kinase activity ratioed to the total CheA or accessible receptor concentration and then normalized to the ratio of Tsr-IM-in vitro lacking (−) attractant (attr). [c] Not detectable.

enabling direct comparison of signaling capabilities of the three complexes.

Notably, the two signaling complexes reconstituted in vitro exhibited 3−4-fold larger relative kinase activities per total CheA than the complex isolated ex vivo (Table 1). This discrepancy suggests that the ex vivo complex possesses an artificially high total CheA concentration, likely arising from unbound, low-activity CheA trapped inside vesicles during isolation. By contrast, the in vitro complexes possess no trapped CheA because their membranes are isolated from *E. coli* strains lacking CheA. Support for this picture is provided by the observation that the in vitro and ex vivo complexes display the same relative kinase activities, within error, per accessible receptor. These findings suggest that the accessible receptor concentration defines the concentration of CheA molecules that can be functionally incorporated into the active signaling complex.

The CheA:receptor stoichiometries measured here (approximately 1:4 to 1:9) are consistent with previous estimates (*21*, *29*) and raise the possibility that each active CheA dimer may associate with multiple receptor dimers in the signaling lattice. However, the accuracies of such stoichiometries are limited by technical difficulties such as the measurement of unpurified receptor concentrations in isolated bacterial membranes.

Finally, the in vitro and ex vivo complexes analyzed herein exhibit receptor positive cooperativities indistinguishable from those previously observed in live cells and in reconstituted complexes (*19*, *20*, *22*, *33*−*35*) as illustrated by the data in Table S1 of the Supporting Information. These similarities suggest that the degree of networking in isolated complexes is similar to the physiological levels of networking that generate receptor cooperativity and pathway ultrasensitivity.

Assembled Signaling Complexes Are Ultrastable in Vitro. We used the basic protocol illustrated in Figure 1 to measure the stability of each signaling complex in vitro under various environmental conditions. Each type of membrane-associated complex was washed to remove unbound components, exposed to a given challenge, and then assayed for the effect of the challenge on complex stability. The different challenges all involved dilution of the complex into a large volume of challenge buffer, followed by incubation for controlled times before washing in assay buffer. Stability assays focused on the retention of CheA by the complex, which was readily measured for all three types of complexes. For the Tsr-IM-in vitro system with its high concentration of inside-out receptors that form accessible complexes, CheA retention could be measured independently in two ways: by its stoichiometry relative to receptor and by its kinase activity. For the Tar-SM-in vitro and Tsr-ex vivo complexes, the receptor expression levels were much lower than for Tsr-IM-in vitro complexes. Moreover, membrane sonication during preparation of the Tar-SM-in vitro and Tsr-ex vivo complexes yielded nearly equimolar populations of inside- and right-side-out receptors, such that only ~50% of the receptor cytoplasmic domains were accessible on the external vesicle surfaces (see Materials and Methods). Thus, relative to the Tsr-IM-in vitro system, the overall levels of accessible complexes were significantly lower for the Tar-SM-in vitro and Tsr-ex vivo systems, making routine quantitations of CheA:receptor ratios imprecise (Table 1) and impractical. However, the stabilities of complexes in the latter two systems could be easily quantitated by their retention of receptor-regulated CheA kinase activity.

First, we tested the kinetic stability of the three signaling complexes in a buffer approximating physiological ionic strength

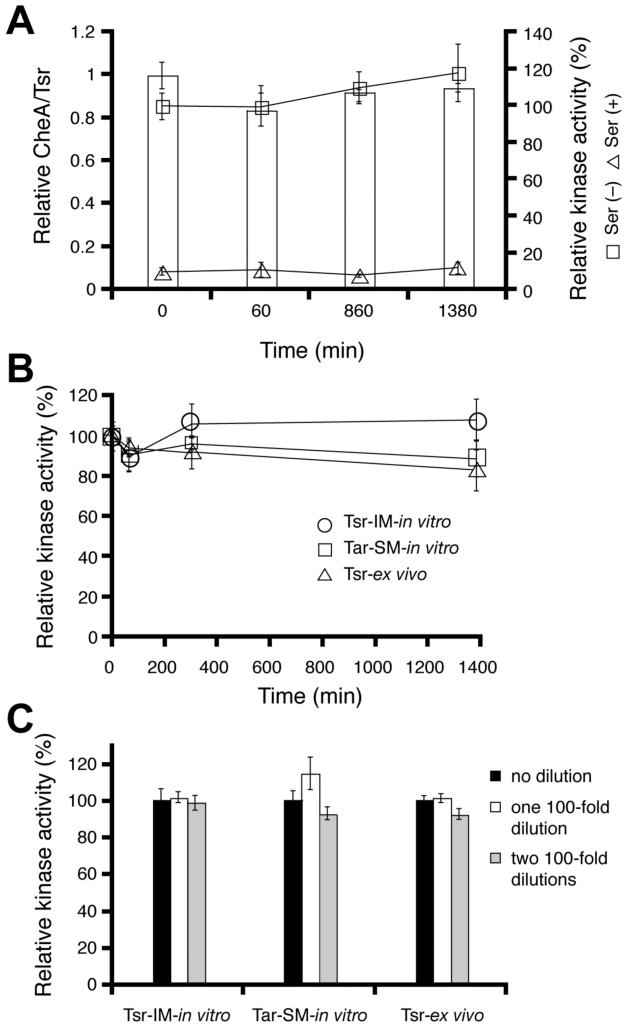

FIGURE 2: Analysis of signaling complex stability. (A) Tsr-IM-in vitro signaling complexes were isolated and diluted 100-fold in activity buffer, incubated for the indicated amount of time, re-isolated, and assayed for retention of receptor-regulated CheA kinase activity in the presence (△) and absence (□) of serine and for retention of CheA by measuring the relative CheA:receptor ratio (white bars). All kinase activities were normalized to the predilution activity in the absence of serine, and all CheA:receptor ratios were normalized to the predilution ratio. (B) Tsr-IM-in vitro (○), Tar-SM-in vitro (□), and Tsr-ex vivo (△) complexes were isolated and diluted 100-fold in activity buffer, incubated for the indicated amount of time, re-isolated, and assayed for retention of receptor-regulated CheA kinase activity. Each kinase activity was normalized to the predilution activity of the corresponding complex. (C) Tsr-IM-in vitro, Tar-SM-in vitro, and Tsr-ex vivo complexes were isolated, and kinase activity was measured without dilution (black bars), after one round of 100-fold dilution and re-isolation (white bars) and after two consecutive 100-fold dilutions and re-isolations (gray bars). Each kinase activity was normalized to the predilution activity of the corresponding complex.

[150 mM NaCl and 5 mM $MgCl_2$ (pH 7.5)]. Each membrane-associated signaling complex was diluted 100-fold and incubated for up to 23 h at 22 °C (Figure 1A, step IV) prior to re-isolation and analysis (Figure 1, steps V and VI). The Tsr-IM-in vitro complex was stable for the entire 23 h (Figure 2), yielding (i) no measurable loss of CheA protein (Figure 2A), (ii) no detectable loss of attractant-dependent, receptor-regulated, CheA kinase activity (Figure 2A), and (iii) no significant loss of CheW protein (Figure 3, right panel and longer time data not shown). The Tar-SM-in vitro and Tsr-ex vivo signaling complexes were equally

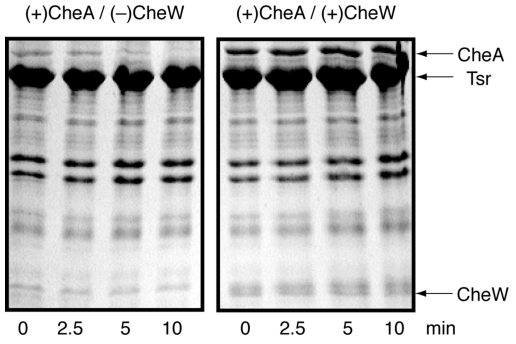

FIGURE 3: CheA and CheW are essential for complex stability. Tsr-IM-in vitro complexes, reconstituted from Tsr and CheA alone (left panel) or from Tsr, CheA, and CheW (right panel), were isolated, resuspended, diluted 100-fold in activity buffer, and re-isolated after the indicated times. Samples were subjected to SDS−PAGE and Coomassie staining.

stable, yielding little or no loss of receptor-stimulated CheA kinase activity during the same 23 h period (Figure 2B). Further experiments demonstrated that all three types of complexes remained stable through repeated cycles of dilution and re-isolation (Figure 2C). Thus, the assembled signaling complex is ultrastable, with a half-life of days or longer regardless of whether assembly occurs in live cells or in vitro.

Such ultrastability requires CheW as well as receptor and CheA. When CheW is omitted during formation of the Tsr-IM-in vitro complex, CheA still binds to the receptor as previously shown (*36*), although the CheA:receptor ratio is significantly decreased (Figure 3, left panel, relative to the right panel with CheW). The resulting binary complex dissociates within minutes of dilution, leading to rapid loss of CheA from the membranes (Figure 3, left panel). This finding also rules out the possibility that proteins might be artifactually trapped by steric constraints imposed during membrane pelleting, since CheA is free to dissociate if CheW is not present to complete signaling complex assembly.

Ultrastability Prevents Exchange with Free CheA or CheW. To further test the ultrastability of assembled signaling complexes, a kinase-inactive CheA mutant (CheA H68Q/G470K), in which the substrate histidine is replaced with a glutamine and the ability to hydrolyze ATP is abolished, was used to challenge the three types of complexes. When present during the assembly of either in vitro complex, the inactive mutant successfully competed with active CheA for incorporation into complexes (although its incorporation seems to be slightly less efficient), leading to loss of kinase activity in both systems (Figure 4A). However, if the mutant was added in vast excess (100-fold, relative to active CheA) after the assembly of active complexes, no loss of kinase activity was observed in any of the in vitro or ex vivo systems (Figure 4B). It follows that preformed complexes exhibit little or no exchange of their bound CheA with free CheA under near-physiological buffer conditions at 22 °C. These findings suggest that the previously observed association of [^{3}H]leucine-labeled CheA with preassembled complexes over a period of 30 min (*28*) arose from binding to empty binding sites [as we have been able to confirm directly in the Tsr-IM-in vitro system (data not shown)] rather than from CheA exchange.

A similar experiment was undertaken using CheW as a challenge. It is known that the presence of inadequate or excess CheW during in vitro complex formation leads to lower levels of CheA incorporation and diminished net kinase activity (*28*, *29*,

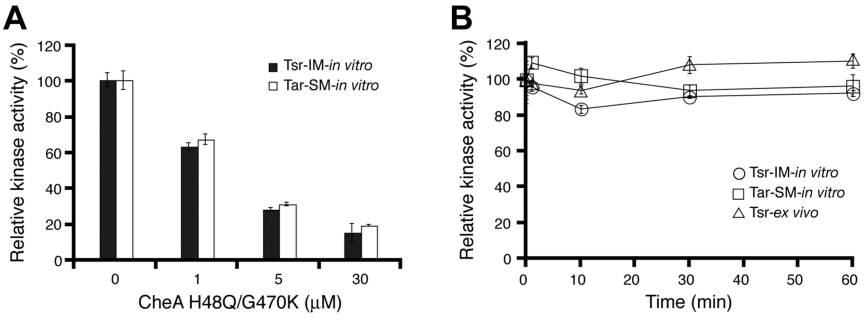

FIGURE 4: Effects of excess kinase-inactive CheA on the signaling complex. (A) Tsr-IM-in vitro (black bars) and Tar-SM-in vitro (white bars) complexes were assembled from receptor-containing membranes, CheW, and active CheA in the presence of increasing amounts of the kinase-dead CheA mutant H48Q/G470K. Kinase activities were measured and normalized to the activity of the complex formed in the absence of the mutant. (B) Preformed Tsr-IM-in vitro (○), Tar-SM-in vitro (□), and Tsr-ex vivo (△) complexes were challenged with 50 μM kinase-dead CheA mutant. Aliquots were removed at indicated time points. Kinase activities were measured and normalized to the activity observed in the absence of the mutant.

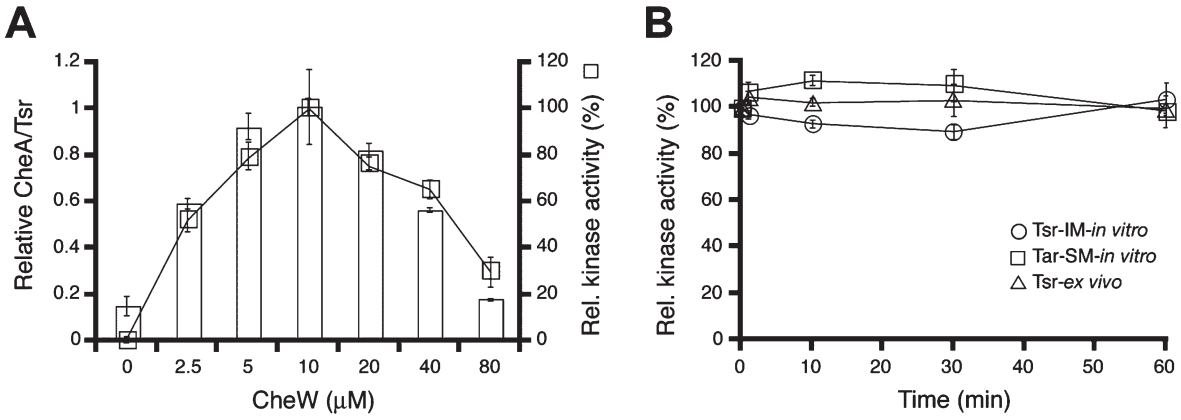

FIGURE 5: Effects of excess CheW on the signaling complex. (A) Tsr-IM-in vitro complexes were assembled from receptor-containing membranes and CheA in the presence of increasing amounts of CheW. Kinase activities and CheA:Tsr ratios were measured and normalized to the highest value. (B) Preformed Tsr-IM-in vitro (○), Tar-SM-in vitro (□), and Tsr-ex vivo (△) complexes were challenged with 50 μM CheW, and aliquots were removed at indicated time points. Kinase activities were measured and normalized to the activity in the absence of CheW. The exchange experiments of Figures 4B and 5B were performed without pelleting the assembled signaling complexes after reconstitution. Thus, the observed lack of exchange cannot be attributed to protein trapping during membrane pelleting. The same results were observed if the signaling complexes were pelleted and resuspended before the addition of excess free kinase inactive CheA or CheW (data not shown).

37). Similarly, under- or overexpression of CheW in vivo inhibits the chemotactic ability of *E. coli* (*38*−*40*). Thus, there is an optimal CheW concentration for signaling complex assembly and function. The inhibitory effect of excess CheW is proposed to arise from the simultaneous binding of two different CheW molecules to the CheW binding sites on the receptor and CheA, thereby competitively inhibiting the normal bridging function of a single CheW bound to these sites (*28*, *38*, *41*). Alternatively, it has been suggested that excess CheW competes with CheA for the latter's binding sites on the receptor (*29*) or inhibits the formation of receptor trimers of dimers in vivo (*42*). In this study, titration of the CheW concentration during in vitro complex assembly yielded a clear optimum in both the CheA incorporation and net kinase activity of the Tsr-IM-in vitro system (Figure 5A). These findings provide additional support for a competitive role for excess CheW during signaling complex assembly. By contrast, if excess CheW (100-fold higher than the assembly concentration) was added after assembly, no effect was seen on the kinase activity of any of the three preformed complexes, indicating a lack of measurable CheW-induced inhibition (Figure 5B). This finding contrasts with a previous study in which excess CheW was found to disrupt the kinase activity of soluble ternary complexes formed from receptor fragments (*43*). Moreover, with regard to general stability, these soluble complexes (*43*, *44*), as well as complexes assembled from receptor fragments on bilayer surfaces (*45*), exhibit dissociation half-lives significantly shorter than those observed here for native complexes. Overall, in contrast to complexes assembled from receptor fragments, membrane-associated signaling complexes assembled from full-length receptors are ultrastable and do not exchange components with aqueous pools of CheA or CheW, providing further evidence that the bound components dissociate extremely slowly.

Ultrastability Can Be Disrupted by Electrostatic Repulsion. To improve our understanding of the extraordinary stability of the signaling complex, we investigated its sensitivity to environmental conditions. First, we tested the effects of ionic strength and pH on stability by varying the buffer in the major dilution step of the standard protocol (Figure 1, step IV). After an incubation period of 45 min in standard or altered buffer, the membrane-associated signaling complexes were sedimented, the supernatant was discarded, and the complexes were resuspended in standard activity buffer. Finally, the complexes were assayed for their CheA:Tsr ratio (Tsr-IM-in vitro system) or kinase activity (all three systems) as measures of stability.

We found that exposure of the preformed complexes to a low ionic strength was highly destabilizing. Such destabilization was apparent as a decreased CheA:Tsr ratio in the Tsr-IM-in vitro system upon exposure of purified, preformed complexes to low-

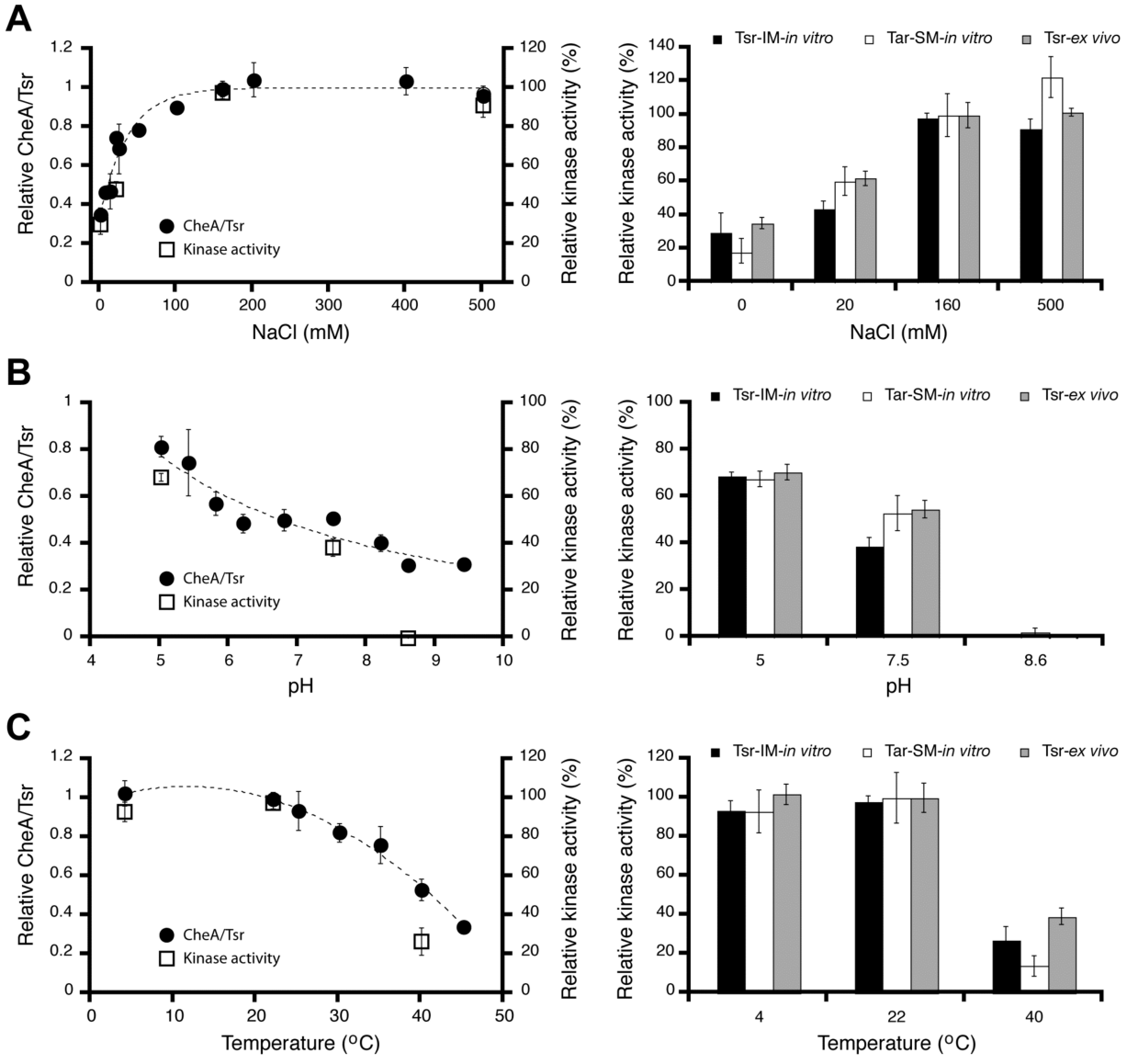

FIGURE 6: Effects of environmental conditions (counterions, pH, and temperature) on signaling complex stability. (A) In the left panel, Tsr-IM-in vitro complexes were isolated and challenged by 100-fold dilution into buffer with the indicated salt concentration. After a 45 min incubation at 22 °C, the complexes were re-isolated, resuspended in activity buffer, and assayed for retention of CheA by measurement of their relative CheA:receptor ratio (●) or their receptor-stimulated kinase activity (□). The CheA:Tsr ratio and the kinase activity were normalized to the values observed for standard buffer conditions [160 mM NaCl (pH 7.5)]. In the right panel, Tsr-IM-in vitro (black bars), Tar-SM-in vitro (white bars), and Tsr-ex vivo (gray bars) complexes were isolated, resuspended, and challenged by 100-fold dilution into buffer at the indicated salt concentration. After incubation for the indicated times, the complexes were re-isolated, resuspended in activity buffer, and assayed for retention of CheA kinase activity. Activities were normalized to the predilution activity of the different complexes. (B) In the left panel, Tsr-IM-in vitro complexes were isolated and challenged by 100-fold dilution into buffer containing 20 mM NaCl at the indicated pH. Complexes were incubated, re-isolated, resuspended, and assayed for their relative CheA:receptor ratio (●) or their receptor-stimulated kinase activity (□). The CheA:Tsr ratio and the kinase activity were normalized to the values observed for standard buffer conditions [160 mM NaCl (pH 7.5)]. In the right panel, Tsr-IM-in vitro (black bars), Tar-SM-in vitro (white bars), and Tsr-ex vivo (gray bars) complexes were isolated, resuspended, and challenged by 100-fold dilution into buffer containing 20 mM NaCl at the indicated pH. After incubation for 45 min, the complexes were re-isolated, resuspended in activity buffer, and assayed for retention of CheA kinase activity. Each activity was normalized to the predilution activity of the corresponding complex. (C) In the left panel, Tsr-IM-in vitro complexes were isolated and challenged by 100-fold dilution into buffer standard buffer at the indicated temperature. Complexes were incubated, re-isolated, resuspended, and assayed for their relative CheA:receptor ratio (●) or their receptor-stimulated kinase activity (□). The CheA:Tsr ratio and the kinase activity were normalized to the values observed for standard buffer conditions [160 mM NaCl (pH 7.5)]. In the right panel, Tsr-IM-in vitro (black bars), Tar-SM-in vitro (white bars), and Tsr-ex vivo (gray bars) complexes were isolated, resuspended, and challenged by 100-fold dilution into standard buffer at the indicated temperature. After incubation for 45 min, the complexes were re-isolated, resuspended in activity buffer, and assayed for retention of CheA kinase activity. Each activity was normalized to the predilution activity of the corresponding complex.

salt conditions [Figure 6A (●)], indicating loss of CheA from the complex. At the same time, a similar loss of receptor-stimulated kinase activity was observed [Figure 6A (□)]. Stability was fully rescued by the inclusion of adequate concentrations of metal ions during the incubation: for example, 100 mM NaCl (Figure 6) or one of 100 mM KCl or 2.5 mM $MgCl_2$, $CaCl_2$, $NiCl_2$, or $BaCl_2$ (data not shown). The ability of diverse metal ions to stabilize the complex indicates that stabilization does not require cation binding to a highly specific site. Instead, the simplest explanation is that the cations effectively shield the repulsive interactions between negative charges on the surfaces of different proteins (see Discussion). To further test this electrostatic destabilization

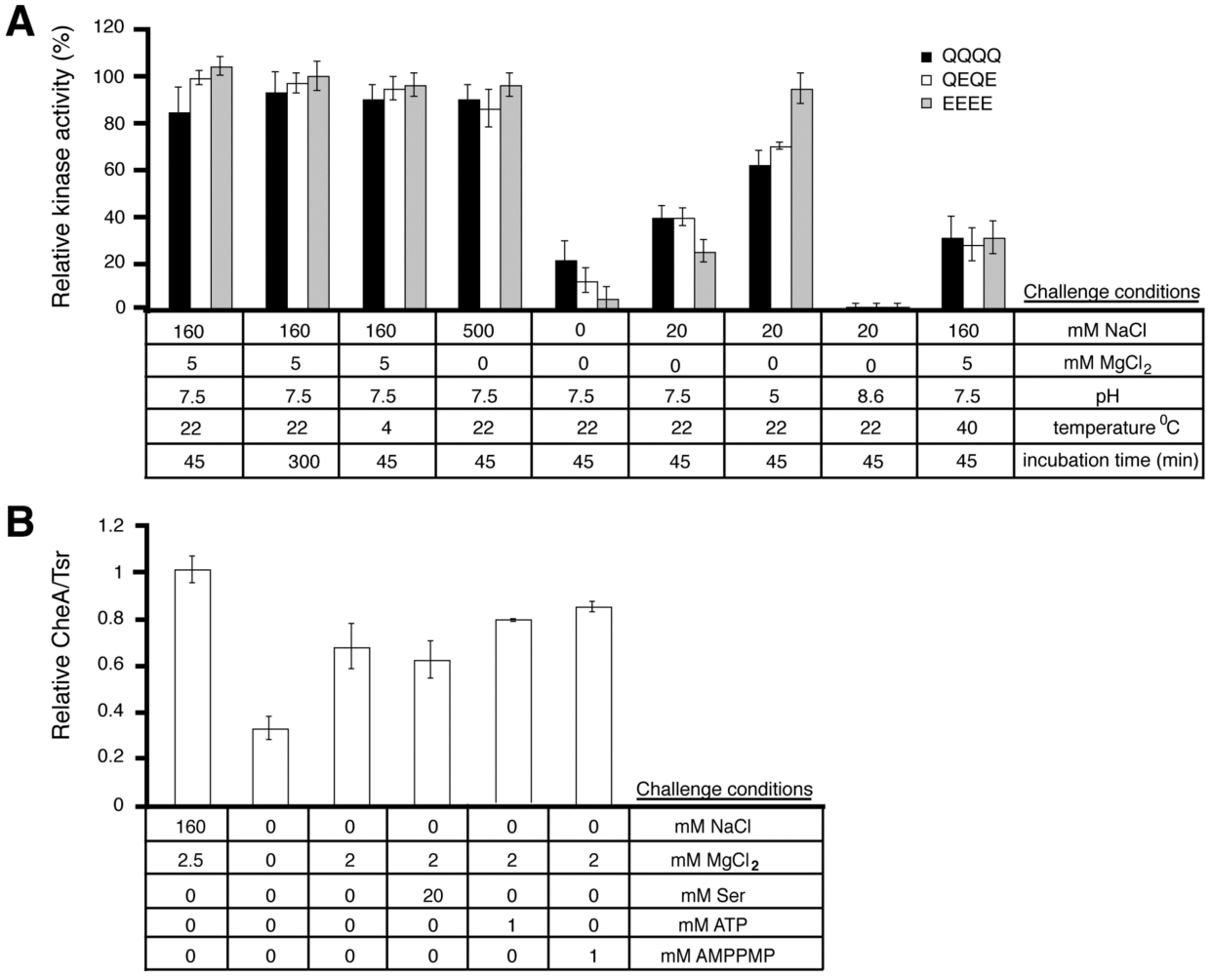

FIGURE 7: Effects of signaling states, ligands, and substrates on signaling complex stability. (A) Tsr-IM-in vitro complexes were prepared from receptors in the QQQQ (black), QEQE (white), or EEEE (gray) adaptation state. The resulting complexes were isolated, resuspended, and diluted in buffer of the indicated composition. Complexes were re-isolated after incubation for 45 min at 22 °C and resuspended in activity buffer. The complexes were assayed for retention of CheA kinase activity, and each resulting activity was normalized to that observed for the corresponding complex under standard conditions [160 mM NaCl and 5 mM $MgCl_2$ (pH 7.5) at 22 °C with a 45 min incubation]. (B) Standard Tsr-IM-in vitro complexes were isolated, resuspended, and challenged by 100-fold dilution into the indicated buffer at pH 7.5 and 22 °C. After a 45 min incubation, the complexes were re-isolated and assayed for retention of CheA by measurement of their relative CheA:receptor ratios, normalized to the ratio observed for dilution in standard buffer containing 160 mM NaCl and 5 mM $MgCl_2$.

hypothesis, we challenged the preformed complexes with an intermediate salt concentration at different pH values. Low pH (5.0) rescued stability, while high pH (8.6) yielded additional destabilization (Figure 6B), strongly supporting the importance of negative surface charges in destabilization. Notably, when complexes challenged with a low ionic strength were tested in kinase assays, they generally lost kinase activity approximately in proportion to the amount of CheA lost from the complex, indicating that most of the surviving CheA was active (Figure 6A). By contrast, treatment with high pH eliminated kinase activity despite partial retention of CheA in the pellets (Figure 6B), suggesting that pH values above 8 may induce some CheA molecules to be inactivated within the complexes. Essentially the same effects of ionic strength and pH were observed in all three types of complexes (Figure 6A,B, right panels), providing additional evidence that the complexes share the same fundamental properties.

Temperature challenges revealed that all three complexes were stable at a low temperature (4 °C) but became unstable at a higher than physiological temperature (40 °C) (Figure 6C, right panel). A temperature titration (Figure 6C, left panel) indicates that temperatures above 35 °C partially inactivate the complex. As observed for high pH, at least some of the inactivated CheA is retained in the pellets, suggesting that high temperatures may induce part of the CheA population to become inactivated within the complexes.

Ultrastability Is Independent of Signaling State. In principle, different signaling or functional states could modulate the stability of the assembled signaling complex. For example, the receptor undergoes transmembrane conformational changes when attractant binds to its periplasmic domain (*13*−*15*, *25*, *46*−*53*) or when its cytoplasmic adaptation sites are covalently modified by adaptation enzymes (*1*, *5*, *54*, *55*). Moreover, CheA can exist in apo or ATP-bound states, and its P1 substrate domain can be unmodified or phosphorylated. The data in panels A and B of Figure 7 indicate that attractant binding and covalent adaptation have no little or no effect on complex ultrastability. A small but reproducible effect is observed for the EEEE adaptation state, wherein kinase activity is found to be more inhibited by a low ionic strength and high pH than observed for less highly charged adaptation states. However, it is likely this inhibition arises from electrostatic destabilization of helix packing within

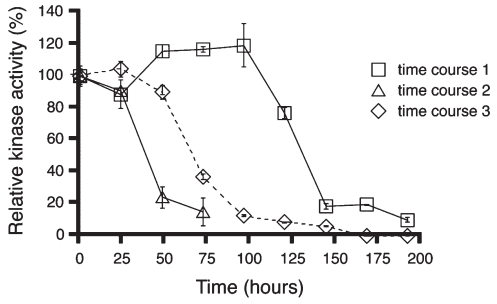

FIGURE 8: Half-life of the signaling complex. Tsr-IM-in vitro signaling complexes were isolated and diluted 100-fold in activity buffer, incubated for the indicated amount of time, re-isolated, and assayed for retention of receptor-stimulated CheA kinase activity. The results of three independent experiments are shown: (□) time course 1, (△) time course 2, and (◇) time course 3. Each kinase activity was normalized to the predilution activity in the same time course.

individual dimers, not from disassembly of the signaling complex. Previous studies have shown that helix packing in the adaptation region of the dimer is electrostatically destabilized by the EEEE state, an effect that would be enhanced at low ionic strength or high pH (*21*, *54*, *56*). Such destabilization is known to inhibit CheA kinase activity, thereby explaining the observed inhibition of EEEE under these conditions. Finally, Figure 7B shows that upon addition of ATP or the nonhydrolyzable ATP analogue ANP-PNP no loss of ultrastability is detected, despite the phosphorylation of the P1 substrate domain by ATP or the introduction of additional negative charges by the bound ATP analogue. Overall, while it remains possible that the receptor signaling state has an undetected, quantitative effect on the signaling complex half-life, it is clear that the complex remains ultrastable in all signaling states tested.

Studies of Signaling Complex Half-Life. Long-term experiments monitoring the core proteins and receptor-stimulated kinase activity of the Tsr-IM-in vitro complex were conducted in an attempt to measure the signaling complex half-life. The findings confirm that the complex remains consistently stable for the first 24 h following assembly (Figure 8; see also Figure 1 above). Subsequently, as soon as 36 h following assembly or as late as 100 h following assembly, the kinase activity begins to decrease. The variable time of inactivation onset is consistent with a cooperative process in which individual complexes begin to become inactivated more rapidly after a threshold level of missing or defective components is reached. Once inactivation begins, the inactivation process takes 12−24 h. The time scale of activity loss presumably reflects the heterogeneous behaviors of the slightly different, individual complexes in the same sample. Such individual complexes may reach the inactivation threshold at slightly different times and may go through the inactivation process at slightly different rates, thereby significantly broadening the inactivation time scale. While in the simplest case the observed kinase inactivation could stem directly from dissociation of CheA from the complex, more complicated inactivation mechanisms such as component denaturation or proteolytic degradation cannot yet be ruled out. Overall, the longest half-life of activity observed thus far is approximately 125 h [5.2 days (Figure 8)].

DISCUSSION

In the bacterial chemotaxis pathway, the signaling lattice formed by the assembly of receptors, CheA, and CheW provides the transmembrane regulation of kinase activity required for cellular responses to extracellular attractants and repellents (*1*). It has been generally assumed in the field that this supermolecular signaling complex is moderately stable, with a dissociation half-life on the order of 10 min in vitro (*28*, *43*), or even more than 30 min (*29*). However, no systematic study of signaling complex stability in vitro has been conducted, and no current model proposes that the signaling complex is ultrastable on the time scale of hours or days.

The findings presented here show that when the signaling complex is analyzed in vitro, under conditions approximating physiological ionic strength, pH, and temperature, it possesses a half-life of days or longer. Three different types of signaling complexes were studied, two assembled from full-length *E. coli* and *S. typhimurium* core proteins in vitro and the third assembled from full-length *E. coli* core components in vivo. All three were isolated in *E. coli* membranes and exhibited well-regulated kinase activities that were strongly inhibited by attractant binding to the receptor, indicating retention of full receptor−kinase coupling with normal transmembrane signaling. For stability studies, one of the two in vitro complexes was well-suited for quantitation of protein retention after various challenges, while all three complexes were well-suited for analysis of kinase activity retention after challenges. Remarkably, when diluted >100-fold in a physiological buffer, the membrane-bound signaling complex exhibited full retention of CheA protein, CheW protein, and CheA kinase activity for at least 24 h at 22 °C. If challenged during assembly, complexes could be inactivated by excess kinase-dead CheA mutant or by excess CheW. Following assembly, however, these challenges had no effect. Overall, the evidence indicates that once the signaling complex is fully assembled from the three core components, it is ultrastable and exhibits no detectable loss of component proteins, no detectable loss of receptor-regulated kinase activity, and no detectable exchange with excess free components for at least a day.

Longer-term experiments suggest that the population of complexes within a given sample eventually begins to inactivate from 1.5 to 4 days after assembly (Figure 8). Further studies are needed to determine the mechanism (denaturation, degradation, dissociation, etc.) of this inactivation and the basis of its variable onset. One possibility is that the highly networked array begins to inactivate in a cooperative fashion after a threshold of nonfunctional or missing components is attained. Such a threshold could be reached earlier by populations of poorly assembled arrays, thereby explaining the variable onset. Regardless of the mechanism of inactivation, it is clear that the half-life of the complex can extend to 5.2 days or perhaps longer. For perspective, this half-life is longer than that of the streptavidin−biotin complex [3.2 days (*57*)], a simple protein−ligand pair that does not form arrays, but is much shorter than that of two-dimensional arrays formed by bacteriorhodopsin in its native cell membrane [more than 20 years (R. Bogomolni and J. Lanyi, personal communications)]. The bacteriorhodopsin example illustrates the power of a simple, highly regular, closely packed array to stabilize protein structure and activity. The chemotaxis signaling complex is formed of multiple protein components, and its array is less regular and more loosely packed (*7*) than that of bacteriorhodopsin (*58*); thus, it is not surprising that it is less stable. To the best of our knowledge, however, the chemotaxis signaling complex is the most stable, multiprotein enzyme complex described thus far.

Different signaling states do not significantly reduce the complex stability, but the complex can be dissociated by non-

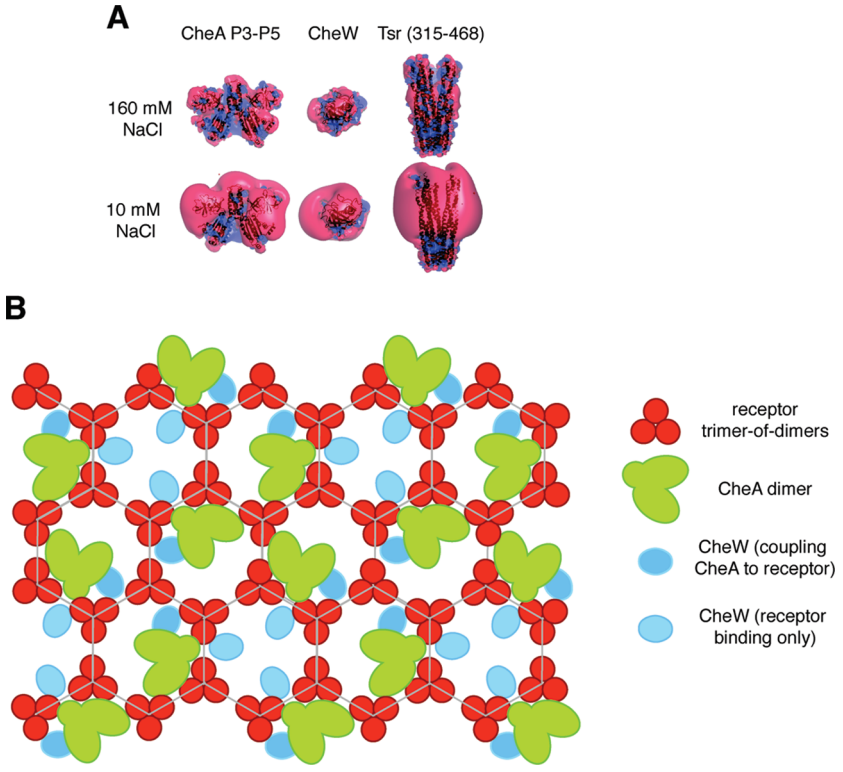

FIGURE 9: Working models. (A) Electrostatic repulsion model for complex dissociation at low ionic strength and high pH. Shown are isopotential contours for ±1 kT/e calculated using the Adaptive Poisson−Boltzmann Solver (APBS) (*67*) and visualized using PyMol (W. L. DeLano, DeLano Scientific) for the *S. typhimurium* CheA P3−P4 domain dimer [modeled on the basis of the structure of the CheA P3−P5 domain dimer from *Thermotoga maritima* (*68*)], for *S. typhimurium* CheW [modeled on the basis of the structure of *E. coli* CheW (*69*)], and for the trimer-of-dimers structure of the cytoplasmic fragment of *E. coli* Tsr (*64*). Red is negative, and blue is positive. The contours in the top panel were calculated in the presence of 150 mM NaCl (pH 7); the contours in the bottom panel were calculated in the presence of 10 mM NaCl (pH 7). (B) Current working model for the lattice structure of the signaling complex illustrating how the receptor lattice, CheA, and CheW might together generate ultrastability. The model shows a cross section, parallel to the plasma membrane and viewed from the membrane looking into the cell, through the signaling array at the height of the receptor−protein interaction domain. Receptor trimers of dimers are colored red, CheA dimers green, CheW molecules that bridge CheA and receptor dark blue, and CheW molecules that interact only with receptor light blue. In the CheA dimer, the small lobe represents the dimer-stabilizing P3−P3′ four-helix bundle. Each large lobe is the P4−P5 region of one subunit where the two subunits are made asymmetric by their different interactions in the complex.

physiological buffer conditions. Thus, when conformational signals are generated within the preformed complex by the addition of modulators or substrates (attractants, ATP, or nonhydrolyzable ATP analogues) or with a change in the receptor adaptation state, no loss of stability is detected. The latter finding supports the conclusion of previous in vitro and in vivo studies that signaling complex architecture is largely unaffected by receptor adaptation state (*21*,*59*). By contrast, lowering the ionic strength or raising the pH can rapidly dissociate the complex. Such destabilization is consistent with the highly anionic surface charge distributions of all three component proteins, illustrated by their isopotential contours in Figure 9A. The contours indicate that negative surface charges are effectively shielded at physiological ionic strength (top panel), but when the ionic strength is decreased to 10 mM, much of this shielding is lost, so that the volume of the isopotential contour expands dramatically (bottom panel). The resulting electrostatic repulsion between different proteins or between different receptor dimers in the trimer of dimers, most likely drives dissociation of the signaling complex at low ionic strength or high pH. Such destabilizing conditions would not be encountered in the cellular ionic environment.

Increasing the temperature to 40 °C also dissociates the complex. In some well-characterized strains of *E. coli* and *S. typhimurium*, chemotaxis pathway function and chemotaxis protein expression both decrease substantially as the temperature increases from 30 to 37 °C (*60*, *61*). Possibly the chemosensory pathway is no longer needed when a suitable host is found, in which case the observed instability near host temperature could help facilitate the rapid dismantling of a pathway that has become dispensable. This idea is controversial, however, since some strains can chemotax well at higher temperatures (V. Sourjik, personal communication). Further studies are required to ascertain the physiological role, if any, of the observed temperature dependence of complex stability.

Strikingly, this finding that the signaling lattice isolated in its native bacterial membranes is stable for days or longer in vitro contrasts with a recent FRAP analysis suggesting that the half-life of fluorescent component exchange is 12 min in live cells at 20 °C (*62*). We have ruled out one artifactual explanation for this discrepancy: the same fluorescent CheW−YFP fusion construct employed in the FRAP studies supports complex ultrastability in our in vitro studies (A. H. Erbse and J. J. Falke, data not shown), indicating that the YFP fusion does not significantly destabilize the complexes. Thus, other explanations for the discrepancy must be considered. We speculate that the more rapid exchange observed in vivo arises from a specialized machinery that disassembles complexes, such as chaperones or proteases, and that this machinery is lost upon signaling complex isolation in vitro. Such a disassembly process would be required to prevent

the ultrastable array from growing too large as new components are synthesized and incorporated. Without such a process, the continuously growing, ultrastable array would eventually fill the inner membrane, crowding its many essential protein components and perhaps disrupting its integrity. The disassembly process could also facilitate the recycling of damaged components, which might otherwise accumulate and lead to array inactivation. Currently, however, we cannot rule out the possibility that disassembly results from an intrinsic property of the native inner membrane that is lost in isolated complexes, for example, the transmembrane potential, rather than from a chaperone/proteolysis system.

The ultrastability we have observed provides strong evidence that the core components are held in place by multiple contacts within the lattice organization revealed by recent cryo-EM studies (*7*, *8*), enabling the assembled complex to "snap" into a structure with much greater integrity than is possible in a nonlattice organization. It is not yet clear whether this ultrastability is primarily (i) thermodynamic, arising from ultra-high-affinity component binding, or (ii) kinetic, arising from steric constraints on component dissociation. Ultrastability requires the presence of only the three core chemotaxis proteins: receptor, CheA, and CheW. Structural constraints provided by the full-length, membrane-embedded receptor are essential since receptor fragments yield a complex of lower stability (*43*−*45*). Finally, since association with the receptor lattice locks the CheA and CheW components into place, one would expect that CheA and CheW binding would also stabilize the receptor lattice. Evidence that such stabilization indeed occurs is provided by the observation that the presence of CheA and CheW blocks the exchange of newly synthesized dimers into existing trimers of dimers in vivo (*42*).

Figure 9B presents one of many possible models that illustrate how the receptor lattice, CheA, and CheW might together generate an ultrastable complex. The main impetus behind the development of this model is the current view of component stoichiometries within the complex. Specifically, the CheA:receptor stoichiometry observed herein for signaling complexes washed extensively to remove unbound components is estimated to range from 1:4 to 1:9 (subunit:subunit), in agreement with other studies (*21*, *29*). Previous estimates of the CheW:receptor stoichiometry range more widely, from 1:7 to 4:6 (subunit:subunit) (*29*, *63*). The model of Figure 9B proposes a CheA:receptor stoichiometry of 1:6 and a CheW:receptor stoichiometry of 1:3, both within their estimated ranges. Furthermore, the proposed model incorporates (i) crystal structures of protein fragments revealing the organization of the trimer of dimers (*64*) and of the CheA−CheW complex (*65*), (ii) recent cryo-EM evidence suggesting that multiple of trimers of dimers may share a single CheA dimer (*7*), and (iii) known protein−protein interaction surfaces on each core component (reviewed in ref (*24*)). Notably, the evidence that CheW is present at a higher stoichiometry than CheA (*63*) suggests that two different types of CheW binding sites exist within the complex as illustrated (Figure 9B). Finally, the model hypothesizes that each CheA dimer bridges three receptor trimers of dimers, thereby generating the multiple, interwoven contacts needed for ultrastability. Clearly, further studies are needed to ascertain whether this model, or a different one, best represents the correct structure. Such studies will be facilitated by the ultrastability of the signaling complex, which ensures that probe-labeled components will remain in place during chemical and spectroscopic analyses of protein−protein interactions. Moreover, the fact that complexes reconstituted in vitro and isolated ex vivo display the same characteristics gives us confidence that reconstitution allows the investigation of near-native assemblies.

This study reveals that the chemotaxis signaling complex is ultrastable and defines the environmental parameters required for ultrastability. Further studies are needed to resolve the possible biological functions of ultrastability. In cells, ultrastability (as modulated by the unidentified disassembly process) could help maintain the highly networked array organization needed for receptor cooperativity and pathway ultrasensitivity. Ultrastability could also minimize the population of active ternary complexes that diffuse away from the signaling lattice; such diffusible ternary complexes would generate background noise because they would not be properly regulated by the adaptation and phosphatase enzyme activities localized to the signaling lattice. Finally, ultrastability could itself be critical to pathway function under certain conditions. For example, in times of extreme starvation, protein synthesis could be halted, and the hypothesized chaperone/proteolysis disassembly system could be inactivated. In this hypothetical scenario, as long as sufficient nutrition was available to power the cell at a minimal level, the signaling complex could remain intact for days as the cell searched for a more favorable living environment.

More broadly, the ultrastability and well-documented ultrasensitivity of the signaling lattice are likely to be widely observed features of the ancient, conserved sensory pathways found in motile bacteria (*66*). In addition, these remarkable properties make the bacterial chemosensory signaling complex an attractive platform for engineering new types of ultrastable, ultrasensitive biosensors.

ACKNOWLEDGMENT

We gratefully acknowledge strains, plasmids, and Tsr antibodies provided by Dr. J. S. Parkinson, plasmids provided by Drs. V. Sourjik and H. C. Berg, CheA antibodies provided by Dr. J. B. Stock, and helpful discussions with Drs. J. S. Parkinson and V. Sourjik.

SUPPORTING INFORMATION AVAILABLE

Comparison of the positive cooperativity of the signaling complexes employed in this work with those of previously published complexes (Table S1). This material is available free of charge via the Internet at http://pubs.acs.org.

REFERENCES

(1) Hazelbauer, G. L., Falke, J. J., and Parkinson, J. S. (2008) Bacterial chemoreceptors: High-performance signaling in networked arrays. *Trends Biochem. Sci. 33*, 9–19.
(2) Parkinson, J. S., Ames, P., and Studdert, C. A. (2005) Collaborative signaling by bacterial chemoreceptors. *Curr. Opin. Microbiol. 8*, 116–121.
(3) Wadhams, G. H., and Armitage, J. P. (2004) Making sense of it all: Bacterial chemotaxis. *Nat. Rev. Mol. Cell Biol. 5*, 1024–1037.
(4) Bourret, R. B., and Stock, A. M. (2002) Molecular information processing: Lessons from bacterial chemotaxis. *J. Biol. Chem. 277*, 9625–9628.
(5) Falke, J. J., and Hazelbauer, G. L. (2001) Transmembrane signaling in bacterial chemoreceptors. *Trends Biochem. Sci. 26*, 257–265.
(6) Maddock, J. R., and Shapiro, L. (1993) Polar location of the chemoreceptor complex in the *Escherichia coli* cell. *Science 259*, 1717–1723.
(7) Khursigara, C. M., Wu, X., and Subramaniam, S. (2008) Chemoreceptors in *Caulobacter crescentus*: Trimers of receptor dimers in a partially ordered hexagonally packed array. *J. Bacteriol. 190*, 6805–6810.

(8) Briegel, A., Ding, H. J., Li, Z., Werner, J., Gitai, Z., Dias, D. P., Jensen, R. B., and Jensen, G. J. (2008) Location and architecture of the *Caulobacter crescentus* chemoreceptor array. *Mol. Microbiol. 69*, 30–41.
(9) Zhang, P., Khursigara, C. M., Hartnell, L. M., and Subramaniam, S. (2007) Direct visualization of *Escherichia coli* chemotaxis receptor arrays using cryo-electron microscopy. *Proc. Natl. Acad. Sci. U.S.A. 104*, 3777–3781.
(10) Sourjik, V., and Berg, H. C. (2000) Localization of components of the chemotaxis machinery of *Escherichia coli* using fluorescent protein fusions. *Mol. Microbiol. 37*, 740–751.
(11) Bray, D., Levin, M. D., and Morton-Firth, C. J. (1998) Receptor clustering as a cellular mechanism to control sensitivity. *Nature 393*, 85–88.
(12) Shimizu, T. S., Aksenov, S. V., and Bray, D. (2003) A spatially extended stochastic model of the bacterial chemotaxis signalling pathway. *J. Mol. Biol. 329*, 291–309.
(13) Chervitz, S. A., and Falke, J. J. (1995) Lock on/off disulfides identify the transmembrane signaling helix of the aspartate receptor. *J. Biol. Chem. 270*, 24043–24053.
(14) Chervitz, S. A., and Falke, J. J. (1996) Molecular mechanism of transmembrane signaling by the aspartate receptor: A model. *Proc. Natl. Acad. Sci. U.S.A. 93*, 2545–2550.
(15) Hughson, A. G., and Hazelbauer, G. L. (1996) Detecting the conformational change of transmembrane signaling in a bacterial chemoreceptor by measuring effects on disulfide cross-linking in vivo. *Proc. Natl. Acad. Sci. U.S.A. 93*, 11546–11551.
(16) Borkovich, K. A., Alex, L. A., and Simon, M. I. (1992) Attenuation of sensory receptor signaling by covalent modification. *Proc. Natl. Acad. Sci. U.S.A. 89*, 6756–6760.
(17) Baker, M. D., Wolanin, P. M., and Stock, J. B. (2006) Signal transduction in bacterial chemotaxis. *BioEssays 28*, 9–22.
(18) Sourjik, V. (2004) Receptor clustering and signal processing in *E. coli* chemotaxis. *Trends Microbiol. 12*, 569–576.
(19) Lai, R. Z., Manson, J. M., Bormans, A. F., Draheim, R. R., Nguyen, N. T., and Manson, M. D. (2005) Cooperative signaling among bacterial chemoreceptors. *Biochemistry 44*, 14298–14307.
(20) Sourjik, V., and Berg, H. C. (2004) Functional interactions between receptors in bacterial chemotaxis. *Nature 428*, 437–441.
(21) Bornhorst, J. A., and Falke, J. J. (2003) Quantitative analysis of aspartate receptor signaling complex reveals that the homogeneous two-state model is inadequate: Development of a heterogeneous two-state model. *J. Mol. Biol. 326*, 1597–1614.
(22) Sourjik, V., and Berg, H. C. (2002) Receptor sensitivity in bacterial chemotaxis. *Proc. Natl. Acad. Sci. U.S.A. 99*, 123–127.
(23) Segall, J. E., Block, S. M., and Berg, H. C. (1986) Temporal comparisons in bacterial chemotaxis. *Proc. Natl. Acad. Sci. U.S.A. 83*, 8987–8991.
(24) Miller, A. S., Kohout, S. C., Gilman, K. A., and Falke, J. J. (2006) CheA Kinase of bacterial chemotaxis: Chemical mapping of four essential docking sites. *Biochemistry 45*, 8699–8711.
(25) Miller, A. S., and Falke, J. J. (2004) Side chains at the membrane-water interface modulate the signaling state of a transmembrane receptor. *Biochemistry 43*, 1763–1770.
(26) Chervitz, S. A., Lin, C. M., and Falke, J. J. (1995) Transmembrane signaling by the aspartate receptor: Engineered disulfides reveal static regions of the subunit interface. *Biochemistry 34*, 9722–9733.
(27) Ames, P., Studdert, C. A., Reiser, R. H., and Parkinson, J. S. (2002) Collaborative signaling by mixed chemoreceptor teams in *Escherichia coli*. *Proc. Natl. Acad. Sci. U.S.A. 99*, 7060–7065.
(28) Gegner, J. A., Graham, D. R., Roth, A. F., and Dahlquist, F. W. (1992) Assembly of an MCP receptor, CheW, and kinase CheA complex in the bacterial chemotaxis signal transduction pathway. *Cell 70*, 975–982.
(29) Levit, M. N., Grebe, T. W., and Stock, J. B. (2002) Organization of the receptor-kinase signaling array that regulates *Escherichia coli* chemotaxis. *J. Biol. Chem. 277*, 36748–36754.
(30) DeFranco, A. L., Parkinson, J. S., and Koshland, D. E. Jr. (1979) Functional homology of chemotaxis genes in *Escherichia coli* and *Salmonella typhimurium*. *J. Bacteriol. 139*, 107–114.
(31) Lefman, J., Zhang, P., Hirai, T., Weis, R. M., Juliani, J., Bliss, D., Kessel, M., Bos, E., Peters, P. J., and Subramaniam, S. (2004) Three-dimensional electron microscopic imaging of membrane invaginations in *Escherichia coli* overproducing the chemotaxis receptor Tsr. *J. Bacteriol. 186*, 5052–5061.
(32) Weis, R. M., Hirai, T., Chalah, A., Kessel, M., Peters, P. J., and Subramaniam, S. (2003) Electron microscopic analysis of membrane assemblies formed by the bacterial chemotaxis receptor Tsr. *J. Bacteriol. 185*, 3636–3643.
(33) Bornhorst, J. A., and Falke, J. J. (2001) Evidence that both ligand binding and covalent adaptation drive a two-state equilibrium in the aspartate receptor signaling complex. *J. Gen. Physiol. 118*, 693–710.
(34) Bornhorst, J. A., and Falke, J. J. (2000) Attractant regulation of the aspartate receptor-kinase complex: Limited cooperative interactions between receptors and effects of the receptor modification state. *Biochemistry 39*, 9486–9493.
(35) Li, G., and Weis, R. M. (2000) Covalent modification regulates ligand binding to receptor complexes in the chemosensory system of *Escherichia coli*. *Cell 100*, 357–365.
(36) Levit, M. N., Abramczyk, B. M., Stock, J. B., and Postel, E. H. (2002) Interactions between *Escherichia coli* nucleoside-diphosphate kinase and DNA. *J. Biol. Chem. 277*, 5163–5167.
(37) Ninfa, E. G., Stock, A., Mowbray, S., and Stock, J. (1991) Reconstitution of the bacterial chemotaxis signal transduction system from purified components. *J. Biol. Chem. 266*, 9764–9770.
(38) Liu, J. D., and Parkinson, J. S. (1989) Role of CheW protein in coupling membrane receptors to the intracellular signaling system of bacterial chemotaxis. *Proc. Natl. Acad. Sci. U.S.A. 86*, 8703–8707.
(39) Sanders, D. A., Mendez, B., and Koshland, D. E. Jr. (1989) Role of the CheW protein in bacterial chemotaxis: Overexpression is equivalent to absence. *J. Bacteriol. 171*, 6271–6278.
(40) Boukhvalova, M. S., Dahlquist, F. W., and Stewart, R. C. (2002) CheW binding interactions with CheA and Tar. Importance for chemotaxis signaling in *Escherichia coli*. *J. Biol. Chem. 277*, 22251–22259.
(41) Surette, M. G., Levit, M., Liu, Y., Lukat, G., Ninfa, E. G., Ninfa, A., and Stock, J. B. (1996) Dimerization is required for the activity of the protein histidine kinase CheA that mediates signal transduction in bacterial chemotaxis. *J. Biol. Chem. 271*, 939–945.
(42) Studdert, C. A., and Parkinson, J. S. (2005) Insights into the organization and dynamics of bacterial chemoreceptor clusters through in vivo crosslinking studies. *Proc. Natl. Acad. Sci. U.S.A. 102*, 15623–15628.
(43) Surette, M. G., and Stock, J. B. (1996) Role of α-helical coiled-coil interactions in receptor dimerization, signaling, and adaptation during bacterial chemotaxis. *J. Biol. Chem. 271*, 17966–17973.
(44) Liu, Y., Levit, M., Lurz, R., Surette, M. G., and Stock, J. B. (1997) Receptor-mediated protein kinase activation and the mechanism of transmembrane signaling in bacterial chemotaxis. *EMBO J. 16*, 7231–7240.
(45) Montefusco, D. J., Asinas, A. E., and Weis, R. M. (2007) Liposome-mediated assembly of receptor signaling complexes. *Methods Enzymol. 423*, 265–298.
(46) Falke, J. J., and Koshland, D. E. Jr. (1987) Global flexibility in a sensory receptor: A site-directed cross-linking approach. *Science 237*, 1596–1600.
(47) Butler, S. L., and Falke, J. J. (1998) Cysteine and disulfide scanning reveals two amphiphilic helices in the linker region of the aspartate chemoreceptor. *Biochemistry 37*, 10746–10756.
(48) Ottemann, K. M., Xiao, W., Shin, Y. K., and Koshland, D. E. Jr. (1999) A piston model for transmembrane signaling of the aspartate receptor. *Science 285*, 1751–1754.
(49) Bass, R. B., and Falke, J. J. (1999) The aspartate receptor cytoplasmic domain: In situ chemical analysis of structure, mechanism and dynamics. *Structure 7*, 829–840.
(50) Irieda, H., Homma, M., Homma, M., and Kawagishi, I. (2006) Control of chemotactic signal gain via modulation of a pre-formed receptor array. *J. Biol. Chem. 281*, 23880–23886.
(51) Swain, K. E., and Falke, J. J. (2007) Structure of the Conserved HAMP Domain in an Intact, Membrane-Bound Chemoreceptor: A Disulfide Mapping Study. *Biochemistry 46*, 13684–13695.
(52) Vaknin, A., and Berg, H. C. (2007) Physical responses of bacterial chemoreceptors. *J. Mol. Biol. 366*, 1416–1423.
(53) Vaknin, A., and Berg, H. C. (2008) Direct evidence for coupling between bacterial chemoreceptors. *J. Mol. Biol. 382*, 573–577.
(54) Starrett, D. J., and Falke, J. J. (2005) Adaptation mechanism of the aspartate receptor: Electrostatics of the adaptation subdomain play a key role in modulating kinase activity. *Biochemistry 44*, 1550–1560.
(55) Lai, W. C., Beel, B. D., and Hazelbauer, G. L. (2006) Adaptational modification and ligand occupancy have opposite effects on positioning of the transmembrane signalling helix of a chemoreceptor. *Mol. Microbiol. 61*, 1081–1090.
(56) Levit, M. N., and Stock, J. B. (2002) Receptor methylation controls the magnitude of stimulus-response coupling in bacterial chemotaxis. *J. Biol. Chem. 277*, 36760–36765.

(57) Piran, U., and Riordan, W. J. (1990) Dissociation rate constant of the biotin-streptavidin complex. *J. Immunol. Methods 133*, 141–143.
(58) Henderson, R., Baldwin, J. M., Ceska, T. A., Zemlin, F., Beckmann, E., and Downing, K. H. (1990) Model for the structure of bacteriorhodopsin based on high-resolution electron cryo-microscopy. *J. Mol. Biol. 213*, 899–929.
(59) Liberman, L., Berg, H. C., and Sourjik, V. (2004) Effect of chemoreceptor modification on assembly and activity of the receptor-kinase complex in *Escherichia coli*. *J. Bacteriol. 186*, 6643–6646.
(60) Wang, E. A., Mowry, K. L., Clegg, D. O., and Koshland, D. E. Jr. (1982) Tandem duplication and multiple functions of a receptor gene in bacterial chemotaxis. *J. Biol. Chem. 257*, 4673–4676.
(61) Hazelbauer, G. L., Mesibov, R. E., and Adler, J. (1969) *Escherichia coli* mutants defective in chemotaxis toward specific chemicals. *Proc. Natl. Acad. Sci. U.S.A. 64*, 1300–1307.
(62) Schulmeister, S., Ruttorf, M., Thiem, S., Kentner, D., Lebiedz, D., and Sourjik, V. (2008) Protein exchange dynamics at chemoreceptor clusters in *Escherichia coli*. *Proc. Natl. Acad. Sci. U.S.A. 105*, 6403–6408.
(63) Li, M., and Hazelbauer, G. L. (2004) Cellular stoichiometry of the components of the chemotaxis signaling complex. *J. Bacteriol. 186*, 3687–3694.
(64) Kim, S. H., Wang, W., and Kim, K. K. (2002) Dynamic and clustering model of bacterial chemotaxis receptors: Structural basis for signaling and high sensitivity. *Proc. Natl. Acad. Sci. U.S.A. 99*, 11611–11615.
(65) Park, S. Y., Borbat, P. P., Gonzalez-Bonet, G., Bhatnagar, J., Pollard, A. M., Freed, J. H., Bilwes, A. M., and Crane, B. R. (2006) Reconstruction of the chemotaxis receptor-kinase assembly. *Nat. Struct. Mol. Biol. 13*, 400–407.
(66) Alexander, R. P., and Zhulin, I. B. (2007) Evolutionary genomics reveals conserved structural determinants of signaling and adaptation in microbial chemoreceptors. *Proc. Natl. Acad. Sci. U.S.A. 104*, 2885–2890.
(67) Baker, N. A., Sept, D., Joseph, S., Holst, M. J., and McCammon, J. A. (2001) Electrostatics of nanosystems: Application to microtubules and the ribosome. *Proc. Natl. Acad. Sci. U.S.A. 98*, 10037–10041.
(68) Bilwes, A. M., Alex, L. A., Crane, B. R., and Simon, M. I. (1999) Structure of CheA, a signal-transducing histidine kinase. *Cell 96*, 131–141.
(69) Li, Y., Hu, Y., Fu, W., Xia, B., and Jin, C. (2007) Solution structure of the bacterial chemotaxis adaptor protein CheW from *Escherichia coli*. *Biochem. Biophys. Res. Commun. 360*, 863–867.